TOWARDS NANOGRAM PER SECOND CORIOLIS MASS FLOW SENSING

Jarno Groenesteijn[1], *Remco G.P. Sanders*[1], *Remco J. Wiegerink*[1], *Joost C. Lötters*[1,2]
[1]MESA+ Institute for Nanotechnology, University of Twente, Enschede, THE NETHERLANDS
[2]Bronkhorst High-Tech BV, Ruurlo, THE NETHERLANDS

ABSTRACT

We have designed, fabricated and tested a micromachined Coriolis flow sensor which can measure up to 50 µg s^{-1} at a maximum pressure drop of 1 bar with a zero stability of 14 ng s^{-1}, an improvement by a factor 40 compared to current state of the art Coriolis flow sensors. This resolution opens up new fields of applications which could up to now not be measured with Coriolis flow sensors.

INTRODUCTION

When measuring large fluid flows, a Coriolis mass flow sensor is generally the preferred sensor due to its medium independent mass flow measurement. While conventional Coriolis flow sensors are widely used, there are no commercially available micromachined Coriolis flow sensors [1]. The most accurate known micro Coriolis mass flow sensor is capable of measuring from 0.55 µg s^{-1} up to 277 µg s^{-1} [2].

Instead, thermal flow sensors are used for very low flows [3], but these kinds of sensors depend on fluid properties and need calibration for each fluid. Using a Coriolis flow sensor for these flows as well would eliminate the need for calibration for each fluid and allows measurement of unknown fluids, e.g. reaction products. In this work we aim at realizing a Coriolis mass flow sensor that can be used in a range down to the ng s^{-1}.

THEORY AND MODELLING

A Coriolis mass flow sensor consists of a vibrating channel through which a fluid is flowing. The fluid flow will cause a Coriolis force on the channel. In our case, the channel is actuated in a twist mode using Lorentz force actuation. An alternating actuation current i_{act} through metal tracks on top of the channel will, in the presence of a magnetic field B, cause a Lorentz force F_L which vibrates the channel around the twist axis ω_y as shown in Figure 1. A mass flow Φ_m through the channel will induce a Coriolis force F_C according to:

$$F_C = -2L_x(\omega \times \Phi_m), \tag{1}$$

where L_x is the width of the channel window. The Coriolis force excites the swing mode around the swing axis ω_x as shown in Figure 2. The sensor is read out using two capacitive comb-structures of each side of the twist axis at distance x_{comb} as shown in Figure 2. The capacitance of these structures depends on the distance between the comb-fingers of the opposing combs and thus of the out-of-plane movement of the channel (in the z direction). The phase-shift between these two signals is then proportional to $\tan^{-1}\left(\frac{A_{Cor}}{A_{act}}\right)$. Where A_{Cor} and A_{act} are the measured amplitude of the Coriolis and actuation modes.

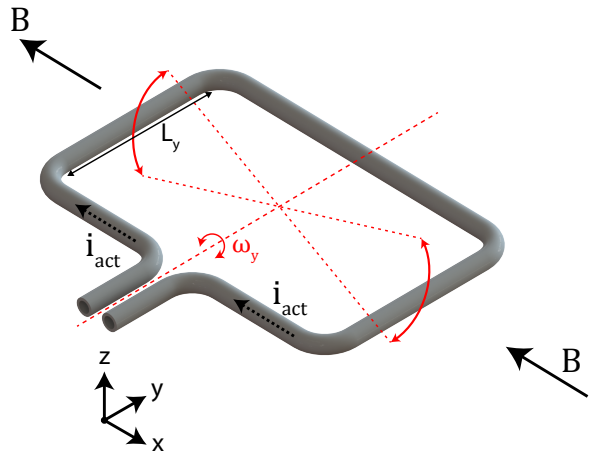

Figure 1: Artist impression of the actuated twist mode of our Coriolis mass flow sensor.

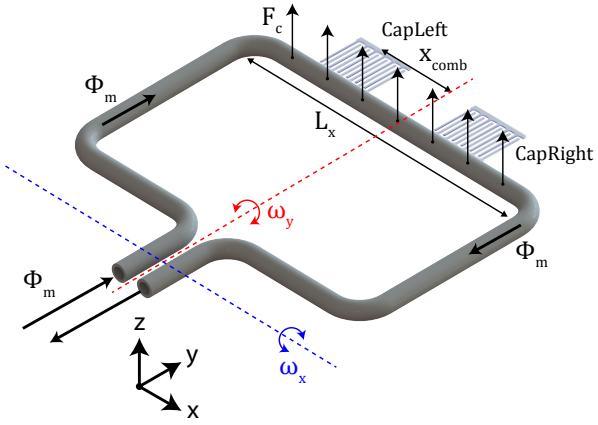

Figure 2: Artist impression of the swing mode of our Coriolis mass flow sensor which is induced by the Coriolis force.

The measured actuation amplitude is proportional on the amplitude of the vibration and on where the comb-structures are located on the channel according to:

$$A_{act} = A_{vibration}\frac{x_{comb}}{0.5L_x}, \tag{2}$$

where $A_{vibration}$ is the amplitude of the vibration and x_{comb} the distance between the centre of the comb-structure and the twist axis. The amplitude of the Coriolis mode is constant for all distances between the comb-structures and twist axis but depends on the Coriolis force given in equation 1

and the swing modes stiffness.

This means that the sensitivity of the sensor to mass flow can be increased using two ways: decreasing the measured actuation amplitude and increasing the measured Coriolis amplitude. Decreasing the measured actuation amplitude can be done by placing the combs closer to the twist axis (reducing x_{comb}). However, increasing the Coriolis amplitude is less straight forward. The motion induced by the Coriolis force can be calculated using the equation of motion of a damped mass-spring system [4]:

$$m\frac{\mathrm{d}^2z(t)}{\mathrm{d}t^2}+c\frac{\mathrm{d}z(t)}{\mathrm{d}t(t)}+kz=F_{\mathrm{C}}(t), \tag{3}$$

where z is the out-of-plane movement and m, c and k are the modal mass, damping and stiffness. Dividing by m and substituting $F_{\mathrm{C}}(t)=|F_{\mathrm{C}}|\cos(\omega t)$ gives:

$$\frac{\mathrm{d}^2z(t)}{\mathrm{d}t^2}+2\zeta\omega_n\frac{\mathrm{d}z(t)}{\mathrm{d}t(t)}+\omega_n^2z(t)=\omega_n^2\frac{|F_{\mathrm{C}}|}{k}\cos(\omega t), \tag{4}$$

where $\zeta=\frac{c}{2\omega_n m}$ is the viscous damping factor and $\omega_n=\sqrt{\frac{k}{m}}$ is the natural frequency. Solving this will lead to an amplitude of [4]:

$$|z(\omega)|=\frac{|F_{\mathrm{C}}|}{k\sqrt{\left[1-(\omega/\omega_n)^2\right]^2+(2\zeta\omega/\omega_n)^2}}, \tag{5}$$

where $|z(\omega)|=A_{\mathrm{Cor}}$ is the frequency dependent Coriolis amplitude, ω is the twist actuation frequency ω_y and ω_n is the swing modes natural frequency ω_x. Since the sensor is actuated at the twist resonance frequency, far from the swing resonance frequency, the contribution of damping $((2\zeta\omega/\omega_n)^2)$ can be neglected.

This shows that the Coriolis amplitude can be increased by increasing the Coriolis force (i.e. increasing the width of the channel window L_{x} or increasing the actuation frequency ω) or by decreasing the denominator in equation 5. This can be done using a numerical multi-axis flexible body model [5] when all geometrical parameters can be changed, or an analytical approximation can be made when only one parameter is variable.

When only the diameter of the channels can be changed and the remaining geometrical parameters (e.g. height (L_{y}) and width (L_{x}) of the channel window) remain constant, the natural frequencies of both the swing and the twist mode are proportional to $\frac{k_m}{m_m}$ with k_m and m_m the modal spring constant and mass. The spring constant depends on the cross-section of the channel and is proportional to d^4 of the channel [6], with d the diameter of the channel. The mass of the whole channel depends on the mass of the tube (proportional to d for very thin channel walls) and the mass of the fluid (proportional to d^2). For liquids, the mass of the fluid will be much higher than that of the channel, resulting in a natural frequency proportional to $\sqrt{\frac{d^4}{d^2}}=d$.

Since both the twist and swing frequency are proportional to the diameter, the only part in the denominator in equation 5 that depends on the diameter is k, which is proportional to d^4. From this can be concluded that the Coriolis amplitude is proportional to d^{-3}, which means that the sensor can be made more sensitive to mass flow by decreasing the channel's diameter.

DESIGN

The two ways to increase the sensitivity to mass flow have both been used.

The measured actuation amplitude has been reduced by reducing the distance between changing the location of the read-out structures. In the previous designs [7, 2], the capacitive comb-structures were placed next to each other as shown in Figure 3a and due to their size, the centre of the combs were 550 µm from the twist axis. By placing the combs on opposite sides of the channel, as shown in Figure 3b, they can partly overlap and the centre of each comb is only 125 µm from the twist axis, resulting in a reduced sensitivity to the actuation mode by a factor $550/125=4.4$.

The measured Coriolis amplitude has been increased by changing the diameter of the channel from 40 µm to 31 µm, resulting in an increase in the Coriolis amplitude by a factor of $(40/31)^3=2.1$, resulting in a total theoretical increase in sensitivity by a factor 9.2.

The electrical noise level of the read-out has also been reduced by increasing the capacitance of the read-out structures. To do this the gap between the comb-fingers of the opposing electrodes has been reduced.

The sensor was fabricated using the fabrication process described in [8]. A photograph of the complete sensor in shown in Figure 4.

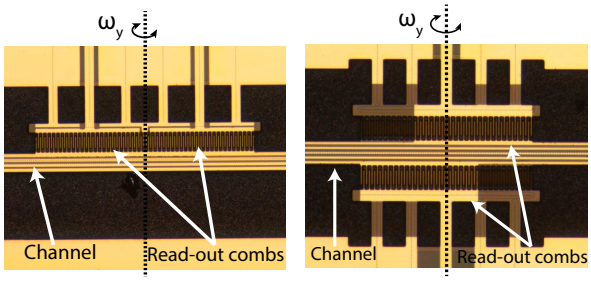

Figure 3: (a) Microscope image of the read-out structures where the combs are located next to each other. (b) Microscope image of the read-out structures where the combs are located on either side of the channel.

FABRICATION

The fabrication process used to fabricate the sensor has been described in [8]. An overview is shown in Figure 5. First, a 500 nm thick layer of LPCVD silicon-rich nitride (SiRN) is deposited on a 525 µm thick silicon wafer. Rectangular etch slits 5 µm long and 1.2 µm wide are etched in the SiRN layer to define the outline of the channels and the channels are etched using a semi-isotropic SF_6 plasma etch (Figure 5a). A thick layer of LPCVD tetraethyl orthosilicate

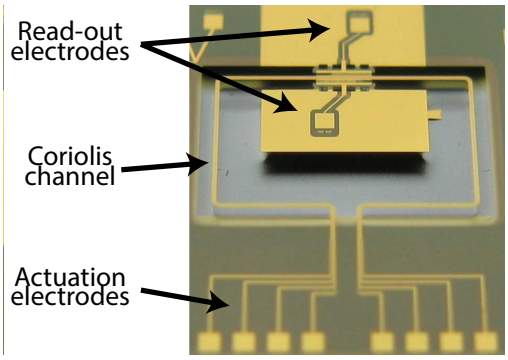

Figure 4: Photograph of the fabricated chip showing the rectangular channel window of the Coriolis sensor and the actuation and read-out electrodes at the top and bottom.

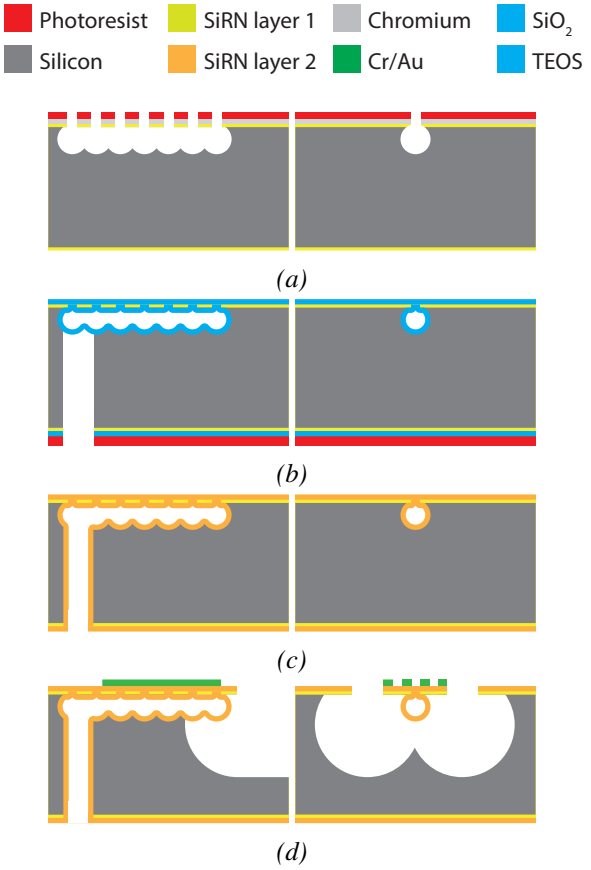

Figure 5: Summary of the fabrication proces used to fabricate the micro Coriolis mass flow sensor.

(TEOS) is deposited to protect the channels during backside processing. The inlets and outlets of the sensor are then etched from the backside using the Bosch process (Figure 5b). The TEOS layer is removed and a thick (1.5 µm) layer of LPCVD SiRN is deposited to form the channel wall and seal the etch slits (Figure 5c). A 10/200 nm thick layer of chromium and gold is sputtered on top of the wafers and patterned to form the tracks and electrodes for actuation and read-out of the chip. The last step consists of an isotropic SF_6 plasma etch step to remove the silicon around part of the channel, resulting in a free-hanging channel that can vibrate (Figure 5d).

EXPERIMENTAL

Measurement Setup

Two different measurements were performed: one to measure performance as a mass flow sensor and one to measure the zero-flow stability and noise level. Figure 6 schematically shows the measurement setup used to measure the sensors performance as a mass flow sensor. A pressurized container, filled with degassed DI water, is connected to the sensor through a 2 µm filter. The output of the sensor is connected to a Bronkhorst µFlow mini flow-controller which can control the flow from 0.5 µg s^{-1} up to 30 µg s^{-1}. During the measurement, the pressure drop over the sensor is measured.

To measure the zero-flow, the channel was filled with DI water and both the inlet and outlet of the sensor were closed. The phase-shift between the two read-out signals is then measured for a period of one hour.

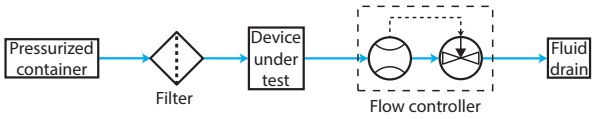

Figure 6: Schematic overview of the measurement setup used to characterise the performance of the sensor as a mass flow controller.

Measurement Results

Figure 7 shows the flow measurement results for a range of 0.5 µg s^{-1} to 30 µg s^{-1}. The measurements are shown with red dots. The dashed line is a linear regression of the measurement points. The sensor shows a linear response over the whole range with a slope of 6 °/(mg/s) which is a factor 9 higher than the sensitivity of the sensor presented by Sparreboom et al. [2]. At 30 µg s^{-1}, the measured pressure drop over the sensor was 600 mbar, indicating a nominal flow (the flowrate at 1 bar pressure drop) of 50 µg s^{-1}.

Figure 8 shows the zero-flow stability measurement over a period of one hour. The red line shows the temperature during this time, while the blue line shows the measurement values calculated to mass flow using the sensitivity measured during the mass flow measurement. The standard deviation on the Coriolis measurement over this period is 0.0011° (indicated with the blue dotted line in Figure 7), equivalent to 14 ng s^{-1}. This is an improvement by a factor 40 compared to the sensor presented by Sparreboom et al. [2], which is in part due to the increase in sensitivity and in part due to a decrease of the noise level due to to large capacitance of the comb-structures.

DISCUSSION

Sensitivity improvements

The increased sensitivity by a factor of 9 is close to the calculated value of 9.2, indicating that the used method to predict the sensitivity is valid. Further decreasing the diameter of the channel will also further increase the sensitivity of the sensor, however, the pressure drop over the sensor is proportional to d^{-4} which means that this methods will

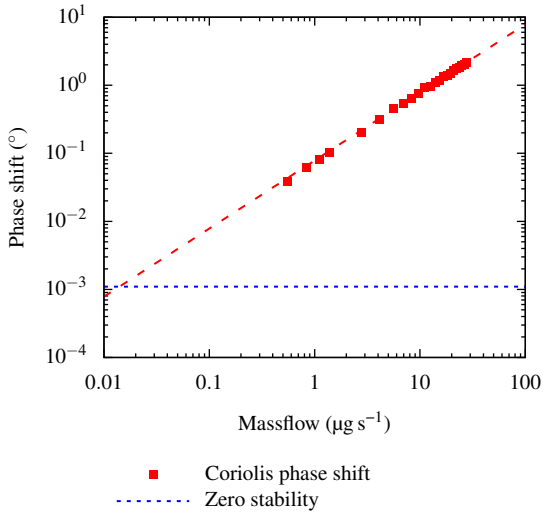

Figure 7: Flow measurement using water. The red dots are measurement points, the red dashed line is a linear regression of the measurement points. The blue dashed line indicates the zero stability of the sensor.

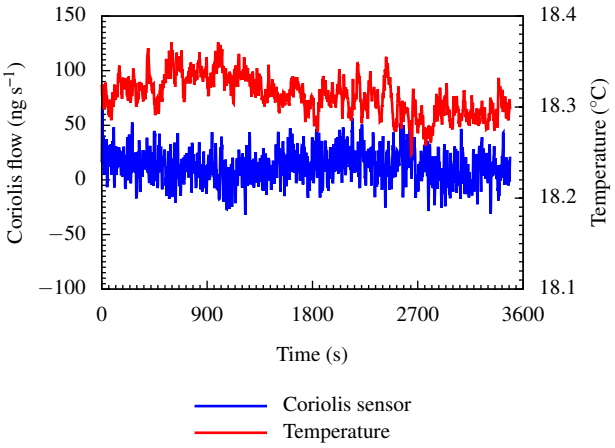

Figure 8: Measured zero stability over a period of one hour (blue line). The temperature is shown in red. The standard deviation of the measurement is 14 ng s^{-1}.

limit the dynamic range of the sensor. At very small diameter, the channel wall will also start having an influence.

The distance between the twist axis and the centre of the comb structures can also be decreased further, however, this also increases the influence of effects that might change the exact location of the twist axis (e.g. imperfections in the fabrication process). Using combs very close to the twist axis in combination with the actuation amplitude cancellation presented by Alveringh et al. [9] can further increase the sensitivity to mass flow.

Measurement setup

The current measurement setup can apply a constant flow between 0.5 µg s^{-1} and 30 µg s^{-1}. However, the noise level at zero flow is much lower than the minimum flow that can be applied. Currently, a setup to reliably apply a flow below 0.5 µg s^{-1} is not available. We will work on improving the measurement setup in order to be able to reliably provide flows down to 1 ng s^{-1}.

CONCLUSIONS

A micro Coriolis mass flow sensor with semi-circular channels with a diameter of 31 µm and a wall thickness of 1.5 µm is presented. The sensor shows a linear response to mass flow and can measure up to 50 µg s^{-1} at a maximum pressure drop of 1 bar. The zero stability of the sensor is 14 ng s^{-1}. Further improvements to the sensitivity will be investigated to bring the zero stability below 1 ng s^{-1}.

ACKNOWLEDGEMENTS

This work is carried out within the Coriolis-based SAS project of NanoNextNL.

REFERENCES

[1] T. Wang and R. Baker, "Coriolis flowmeters: a review of developments over the past 20 years, and an assessment of the state of the art and likely future directions," *Flow Measurement and Instrumentation*, vol. 40, pp. 99–123, Dec 2014.

[2] W. Sparreboom *et al.*, "Compact mass flow meter based on a micro coriolis flow sensor," *Micromachines*, vol. 4, no. 1, pp. 22–33, 2013.

[3] J. T. W. Kuo *et al.*, "Micromachined thermal flow sensors-A review," *Micromachines*, pp. 550–573, 2012.

[4] L. Meirovitch, *Fundamentals of Vibrations*. McGraw-Hill, 2001.

[5] J. Groenesteijn *et al.*, "Modelling of a micro Coriolis mass flow sensor for sensitivity improvement," in *IEEE SENSORS 2014 Proceedings*. Institute of Electrical & Electronics Engineers (IEEE), 2014.

[6] C. W. Young and G. R. Budynas, *Roark's formulas for stress and strain*, L. Hager, Ed. McGraw-Hill, 2002.

[7] J. Haneveld *et al.*, "Modeling, design, fabrication and characterization of a micro Coriolis mass flow sensor," *Journal of Micromechanics and Microengineering*, vol. 20, 2010.

[8] J. Groenesteijn, "Microfluidic platform for Coriolis-based sensor and actuator systems," Ph.D. dissertation, University of Twente, Enschede, Jan 2016. [Online]. Available: http://dx.doi.org/10.3990/1.9789036540117

[9] D. Alveringh *et al.*, "A novel capacitive detection principle for Coriolis mass flow sensors enabling range/sensitivity tuning," in *Proceedings of Micro and Nano Engineering*, 2015.

CONTACT

J. Groenesteijn, +31 53 489 4373,
j.groenesteijn@utwente.nl